STATUS OF INDIUM PHOSPHIDE SOLAR CELL DEVELOPMENT AT SPIRE*

M.B. Spitzer, C.J. Keavney, and S.M. Vernon
Spire Corporation
Bedford, Massachusetts

On-going development of indium phosphide solar cells for space applications is presented. The development is being carried out with a view toward both high conversion efficiency and simplicity of manufacture. The cell designs comprise the ion-implanted cell, the indium tin oxide top contact cell, and the epitaxial cell grown by metal organic chemical vapor deposition. Modelling data on the limit to the efficiency are presented and comparison is made to measured performance data.

INTRODUCTION

The radiation sensitivity of space solar cells is a critical factor affecting many aspects of space power system design, and improvements to end-of-life cell efficiency offer numerous advantages in cost, weight and area. For the large power systems anticipated for future space projects (ref. 1), reduction of array area may be particularly important, owing to weight and drag considerations, and to the necessity of assembly and maintenance in space. This reduction of area is possible if end-of-life efficiency can be increased.

Recently, Yamamoto et al. (ref. 2) have reported that indium phosphide (InP) solar cells have remarkable radiation tolerance. Their results indicate that both electron and x-ray damage are completely annealed at 100°C. A further important result is that the radiation damage is annealed by minority carrier injection (ref. 3,4). These cells would therefore seem to have considerable promise as a new type of radiation-resistant space solar cell.

In the work to be reported here, our objective is first to reproduce the work of Yamamoto et al., and then to examine the generality of the findings regarding radiation tolerance. Our work is also carried out with a view toward high efficiency, and with a secondary goal being the identification of useful manufacturing techniques. The specific devices investigated by us are: (1) the ion-implanted cell, (2) the indium tin oxide (ITO) coated cell, and (3) epitaxial cells formed by metalorganic chemical vapor deposition. By investigating three

* This work is funded by NASA contract NAS3-24857.

manufacturing approaches, we intend to gain an understanding of the efficiency and radiation tolerance for various cell structures, and hence the generality of the findings of Yamamoto et al.

In this paper we will first present a review of our modelling of InP solar cells; this modelling has served as a basis for both cell design and analysis of loss mechanisms. We then present a description of our cell fabrication experiments. At the present time, we have fabricated test solar cells and are working on obtaining improvements in efficiency. Results obtained thus far will be presented.

MODELLING

To identify a high efficiency cell design for InP, we utilized a solar cell modelling code developed at Brown University (ref. 5). This code evaluates the solution of the one-dimensional time-independent inhomogeneous diffusion equation. This solution is integrated over the solar spectrum to determine the terminal characteristics of the device.

The code is based on the partition of the cell into three regions: the emitemitter, the space-charge region, and the base. The boundary conditions are the conventional Boltzmann conditions at the edges of the space-charge region, and the surface recombination velocity at the outside surfaces of the cell. The code also calculates generation in the space-charge region.

A literature search was carried out to determine up-to-date input parameters for the model. Optical data were obtained from reference 6. Data on the AM0 spectrum were obtained from M. Wolf (ref. 7). Mobility data were compiled from various sources, and figure 1 indicates the values used in the modelling. Owing to a lack of experimental data, it was necessary to assume that the minority carrier lifetime is inversely proportional to the majority carrier concentration. For a doping level of 2×10^{16} cm^{-3}, this assumption yields an electron diffusion length (L_e) of about 10 micrometers. At the present time, our assumption appears to be reasonable based on the dependence of lifetime upon doping in other semiconductors. We also assume an emitter doping level of 5×10^{18} cm^{-3} and a space-charge region (SCR) width of 0.25 micrometers. The junction depth is assumed to be 0.2 micrometers. Other parameters used for modelling are provided in table 1.

The model has been used to calculate the limit to the conversion efficiency as a function of resistivity. Since the dependence of L_e upon doping is not well established, we varied L_e over a wide range. The results of this calculation are shown in figure 2. We also have indicated the efficiency for values of L_e consistent with the lifetime given by our assumption that lifetime is inversely in proportional to carrier concentration; this result is shown as data points in the figure. This assumption yields the dashed line in figure 2, which shows that the optimum doping is in the range of 10^{16} cm^{-3} to 10^{17} cm^{-3}. This range is fortunately also approximately optimal for radiation hardness (ref. 8). For this

cell structure, the upper limit to the AM0 efficiency is then 18% (including 8% shadow loss). If higher lifetime can be obtained, AM0 efficiency of up to 20% may be possible.

We have also examined the importance of hole diffusion length (L_h) in the n-type emitter, for a junction depth of 0.1 micrometer. In this calculation, we assume that in the base the acceptor concentration is fixed at 2×10^{16} cm^{-3}. The result of this calculation is shown in figure 3. It can be seen that if L_h can be increased, the upper limit to the efficiency approaches 22%.

The theoretical external quantum efficiency (QE) of InP cells has been investigated to gain an understanding the way that L_e and junction depth (x_j) affect the efficiency of non-ideal experimental cells. Although antireflection (AR) coatings are necessary in the final cells, uncertainties in the optical properties increase the difficulty of the modelling and analysis. For this reason, many of our experiments involve non-coated cells. Therefore, in our QE calculations, measured reflectance of non-AR-coated InP was used to facilitate comparison of theory to actual cell data.

Figure 4 shows the calculated external QE as a function of L_e. It can be seen that varying L_e between 1 and 9.5 micrometer has only a small effect; this is a result of the fact that most of the current is generated in the emitter and space-charge region. For example, if one assumes a junction depth of 0.1 micrometer, one finds that a non-AR-coated cell with L_e=9.5 micrometer should have J_{sc} of 23.8 mA/cm^2. Of this total, only 5.8 mA/cm^2 is generated in the base. The emitter generates 8.7 mA/cm^2. The width of the space charge region is 0.25 micrometer, and 9.34 mA/cm^2 are generated within it. Thus, this modelling indicates the need for high quality near-surface regions. We note that these tentative findings are based on the optical data of reference 6, and that it would be desirable to obtain absorption data from crystals that are grown in the same manner and doped as the solar cells being investigated here.

CELL FABRICATION EXPERIMENTS

Experiments have been carried out on the fabrication of cells. The three cell designs are shown in figure 5. Note that the ion-implanted and ITO-coated cells utilize lightly-doped substrates whereas the epitaxial cell is grown on a p^{++} wafer, which has an orientation of 2° off <100>. The final cell area in our experiments is 0.5 cm x 0.5 cm.

Ion-Implanted Solar Cells

The use of ion implantation for junction formation in InP has received attention (ref. 9-14). Such junctions have been evaluated for application to cell fabrication. Table 2 summarizes the process parameters investigated, as well as the parameters that have yielded the best results thus far. The best parameters shown in the table yield a sheet resistance of 500 ohms-per-square, Hall mobility of 690 $cm^2/Vsec$, and junction depth estimated to be 0.2 micrometers. We have

investigated the use of C-V based junction profiling techniques, but at the present the application to very shallow junctions appears to be unreliable.

Fabrication of cells comprises ion implantation and annealing as shown in table 2. The wafers are then provided with front (Ge-Au) and back (Zn-Au) contacts. A mesa etch is used to separate the junctions. Finally, a multilayer AR coating is applied.

Characterization of the cells indicates that the primary loss mechanism in most of the cells is space-charge region recombination (n=2 over four decades). Quantum efficiency measurements indicate low blue response which may be attributable to either space-charge region recombination or possible emitter recombination (bulk or surface). Further experiments on junction formation are underway to improve the dark characteristics of the device. Nevertheless, AMO efficiency of over 13% has been obtained, as will be discussed in the next section.

ITO-coated Cells

The use of ITO as a top contact has recently gained attention, and highly efficient cells have been reported (ref. 15). We have therefore investigated ITO deposition by RF sputtering with a variety of process conditions. The best ITO films are approximately 0.1 micrometers thick and have sheet resistance of about 180 ohms-per-square. The absorption within the films is negligible in the range of 500 nm to 1000 nm.

Fabrication of cells begins with the formation of the Zn-Au back contact. Next, the ITO is deposited and front contacts are applied. A mesa etch is used to separate the cells. Finally, if desired, a single layer of MgF is applied to reduce reflection.

The best cells are presently characterized by low fill factor (FF) and low open circuit voltage (V_{OC}). The cause of the low performance has not been identified, but it is possibly the result of a high density of interface states which could cause the device to perform as a Schottky diode. Further work in this area is in progress.

Epitaxial Cells

We are presently investigating formation of both grown junctions and complete cells by metalorganic chemical vapor deposition. For the grown junctions, we are using <100> lightly doped p-type substrates, and the desired resultant structure is the same as is shown in figure 5a for the ion-implanted device. As in the ion-implanted cell, a large fraction of the space-charge region is formed in the starting wafer. We are also investigating the all-epitaxial cell shown in figure 5c, in which the emitter and base are formed in epitaxial material grown on a more highly doped photovoltaically-inactive substrate.

The source gases for this work are $(CH_3)_3In$ and PH_3. N-type dopants under evaluation are SiH_4, H_2Se and $(CH_3)_4Sn$. For p-type doping, we are investigating $(CH_3)_2Zn$ and CP_2Mg. The growth temperature is in the range of 600 to 650°C with a pressure of 76 torr.

The solar cell structures that have been investigated to date include thin abrupt homojunctions, graded emitters, and high-low emitters. The highest V_{OC} has been obtained with thin homojunctions, but the best J_{SC} is obtained with the high-low emitters. Further work is underway to better understand the performance of the grown junctions.

CELL PERFORMANCE

We have fabricated cells with each of the processes and designs described above. The ion-implanted cell has thus far yielded the best performance. The best cells of each type are summarized in table 3. It should be noted that the epitaxial cells are the results of our first cell fabrication run, and are rather good for a first attempt.

The illuminated current-voltage characteristic for the best cell is shown in figure 6. We have obtained AM0 efficiency of 13.3%. V_{OC} is 807mV and J_{SC} is 29.6 mA/cm^2. To understand the origin of the loss mechanisms, we measured the dark log current-voltage and V_{OC}-I_{SC} characteristics, shown in figure 7. Analysis shows that the fill factor is limited in part by junction recombination (n=1.7 at Vmp), and in part by series resistance. Calculations show that the ideal fill factor is 86.2%; this is reduced to 82.6% by leakage current, and to 81.8% by series resistance. The combined effects of series resistance and leakage reduce the fill factor to 76.1%. If such effects could be eliminated, efficiency would be raised to 15.3%. Examination of the data also shows that for this cell the V_{OC} is not limited by space-charge region recombination.

Measured external QE data are shown in figure 8. The low blue response indicates that the recombination in the emitter and/or space-charge region is limiting the J_{SC}. Development of improved epitaxial emitter structures is expected to correct this problem.

CONCLUSION

The status of our InP solar cell development has been presented. Efficiency of 13.3% (AM0) has been obtained and the manner in which greater performance could be obtained has been reviewed. It is expected that by improving the minority carrier properties of the emitter and space-charge region, AM0 efficiency of 16% can be achieved in the near future.

REFERENCES

1. Forestieri, A.F. and Baraona, C.R., "Space Station Power System," Rec. of the 17th IEEE Photovoltaic Specialists Conference, Orlando (1984), p. 7.

2. Yamamoto, A.; Yamaguchi, M.; Uemura, C., "High Conversion Efficiency and High Radiation Resistance InP Homojunction Solar Cells," Appl. Phys. Let. 44, 611 (1984).

3. Yamaguchi, M.; Andu, K.; Yamamoto, A.; and Uemura, C., "Minority-Carrier Injection Annealing of Electron Irradiation-Induced Defects in InP Solar Cells," Appl. Phys. Lett. 44, 432 (1984).

4. Yamaguchi,M.; Uemura, C.; and Yamamoto, A., "Radiation Damage in InP Single Crystals and Solar Cells," J. Appl. Phys. 55, 1429 (1984).

5. Spitzer, M.B., "The Upper Limit to the Theoretical Efficiency of P-N Homojunction and Interfacial Layer Heterojunction Solar Cells," Ph.D. Thesis, Brown University (1981).

6. Aspnes and Studinoff, Phys. Rev. B., 27, 985 (1983).

7. Wolf, M., private communication.

8. Yamaguchi, M.; Ando K.; and Uemura, C., "Carrier Concentration Effects on Radiation Damage in InP," J. Appl. Phys. 55, 3160 (1984).

9. Davies, D.E.; Lorenzo, J.P.; and Ryan, T.G., "N-type Doping of Indium Phosphide by Implantation," Solid-State Electronics 21, 981 (1978).

10. Donnelly, J.P. and Ferrante, G.A., "The Electrical Characteristics of InP Implanted with the Column IV Elements," Solid-State Electronics 23, 1151 (1980).

11. Kasahara, J.; Gibbons, J.F.; Magee T.J.; and Perry, J., "Ion Implantation of Sulfur in Cr-doped InP at Room Temperature," J. Appl. Phys. 51, 4119 (1980).

12. Inada, T.; Taka, S.; Yamamoto, Y. "Selenium Implantation in Indium Phosphide," J. Appl. Phys. 52, 4863 (1981).

13. Sussmann, R.S., "N-type Doping of InP by Io Implantation," J. of Elect. Mater. Vol. 12, No. 3, p. 603 (1983).

14. Gouskov, L.; Conjeud, A.L.; Dhouib, A.; Favenec, P.N.; Salvi, M.; L'Haridon, H.; Bastide G. and Bayaa, D., "n^+-InP (Silicon Implanted)/p-InP Homojunction: Minority Carrier Diffusion Length in the Implanted Layer," Solar Cells 11, 343 (1984).

15. Coutts, T. and Naseem, S., "High Efficiency Indium Tin Oxide/Indium Phosphide Solar Cells," Appl. Phys. Lett. 46, 164 (1985).

TABLE 1. MODEL INPUT PARAMETERS

PARAMETER	VALUE
Temperature, T	28°C
Intrinsic Concentration, n_i	2.6×10^7 cm^{-3}
Donor Concentration, N_D	5×10^{18} cm^{-3}
Acceptor Concentration, N_A	2×10^{16} cm^{-3}
Electron Diffusion Length, L_e	9.5 μm
Hole Diffusion Length, L_h	0.08 μm
Electron Mobility	3500 $cm^2/Vsec$
Hole Mobility	60 $cm^2/Vsec$
Input Spectrum	AM0, 135.3 mW/cm^2
Shadow Loss	8%
Reflection Loss	0

TABLE 2. DEVELOPMENT OF ION IMPLANTED JUNCTIONS

PROCESS PARAMETER	RANGE INVESTIGATED	BEST RESULT
Implant Energy (keV)	10 to 50	10
Implant Dose (cm^{-2}) (Si,Se, S)*	3×10^{14} to 10^{15}	10^{15}
Anneal Temp. (°C)	700 to 800	750
Anneal Time (min)*	1 to 15	15
Surface Protection	Flowing PH_3, PSG, Si_3N_4, Silox	Flowing PH_3

*Experiments in progress.

TABLE 3. SOLAR CELL PERFORMANCE DATA FOR THE BEST CELL OF EACH TYPE

Cell Type	V_{oc} (mV)	J_{sc} (mA/cm^2)	FF (%)	Eff (%)
Ion-implanted	807	29.6	75.2	13.3
ITO-coated	689	19.7	62.0	6.2
Epitaxial	721	23.6	73.0	9.2

Notes: AM0, 135 mW/cm^2. T = 25°C. Area = 0.25 cm^2.

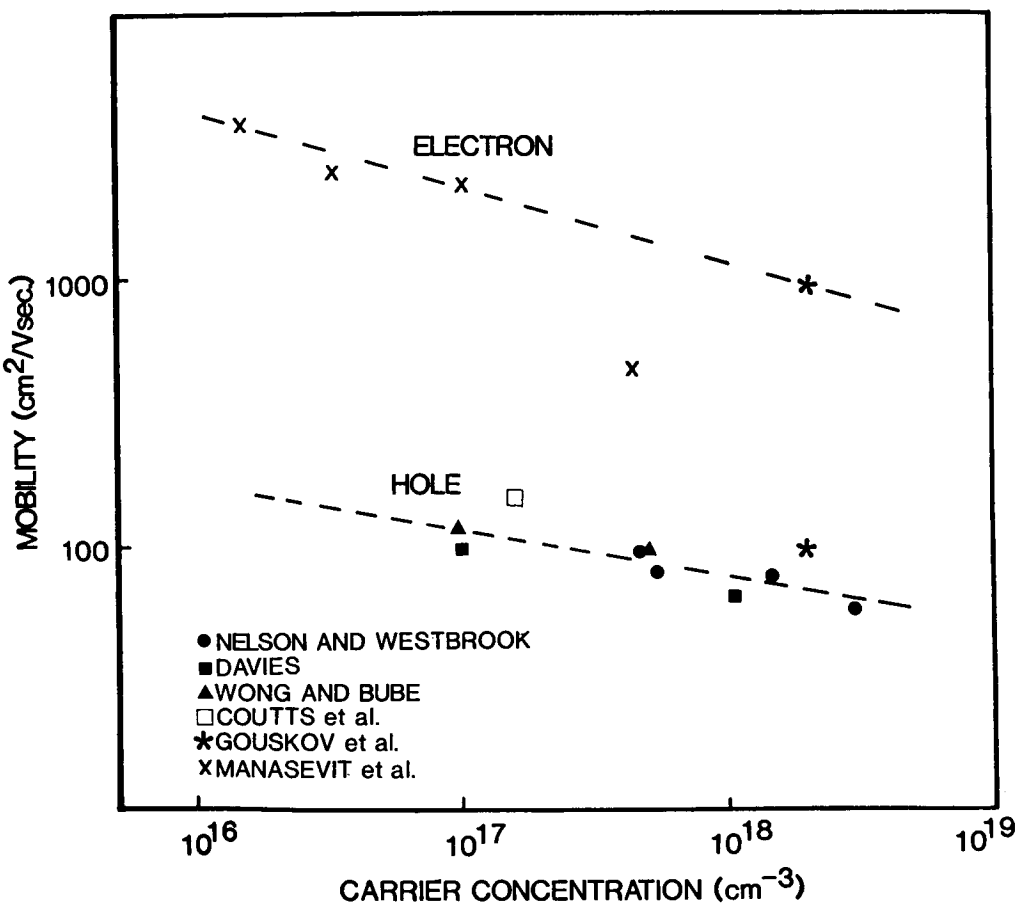

Figure 1. MOBILITY AS A FUNCTION OF CARRIER CONCENTRATION IN InP. The dotted lines indicate the values used in the model.

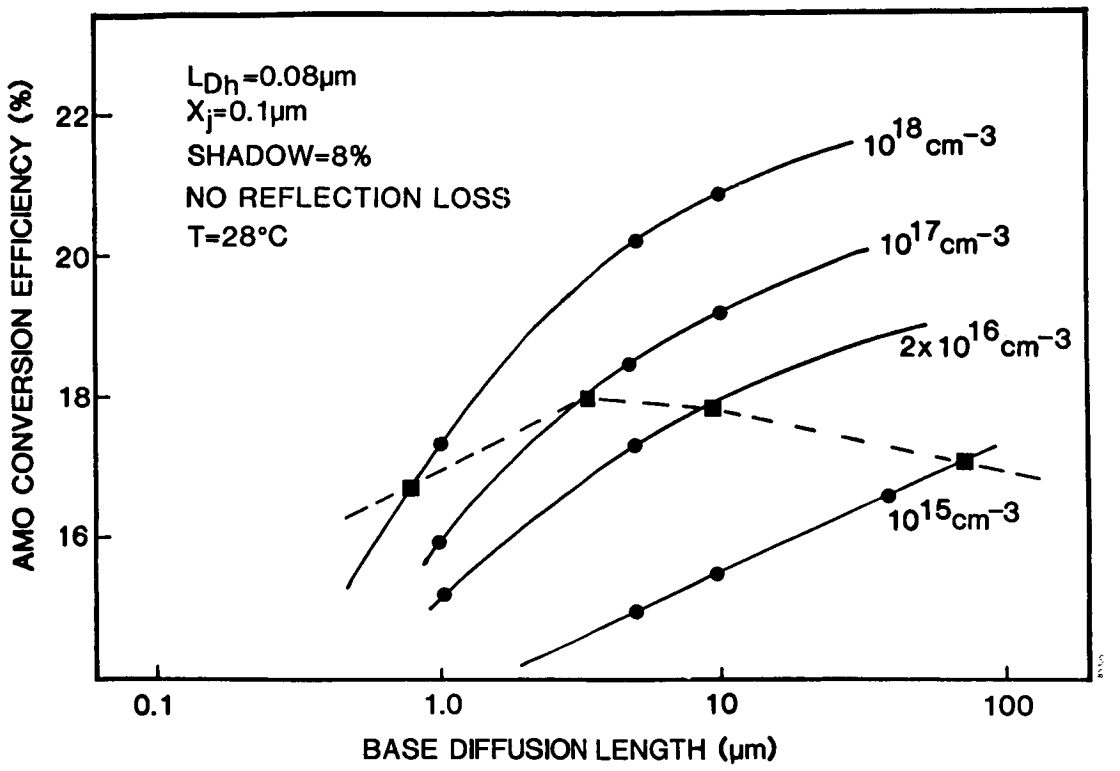

Figure 2. THEORETICAL AMO EFFICIENCY AS A FUNCTION OF L_e AND RESISTIVITY. The dotted line indicates the value of L_e associated with the assumed dependence of lifetime upon dopant concentration.

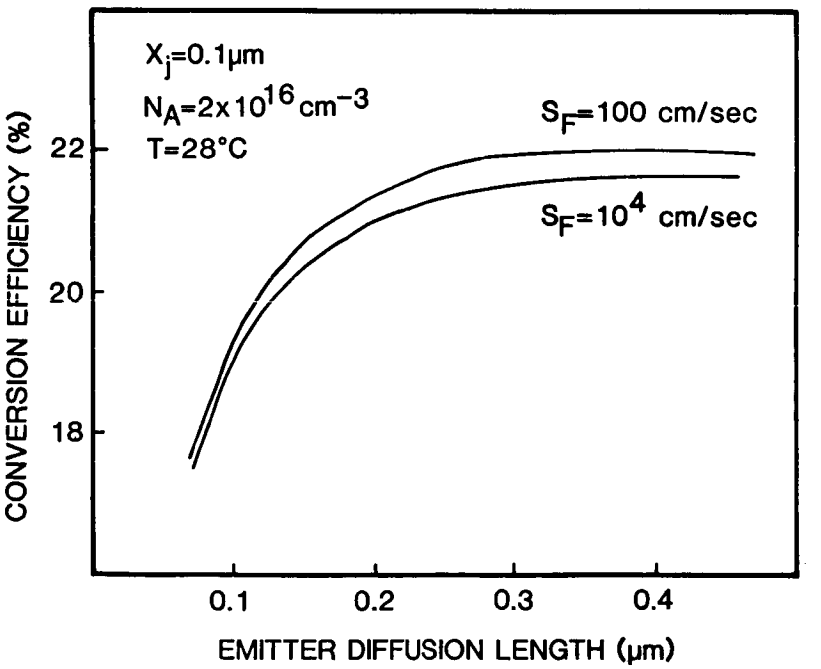

Figure 3. UPPER LIMIT TO THE AMO EFFICIENCY AS A FUNCTION OF HOLE DIFFUSION LENGTH IN THE EMITTER.

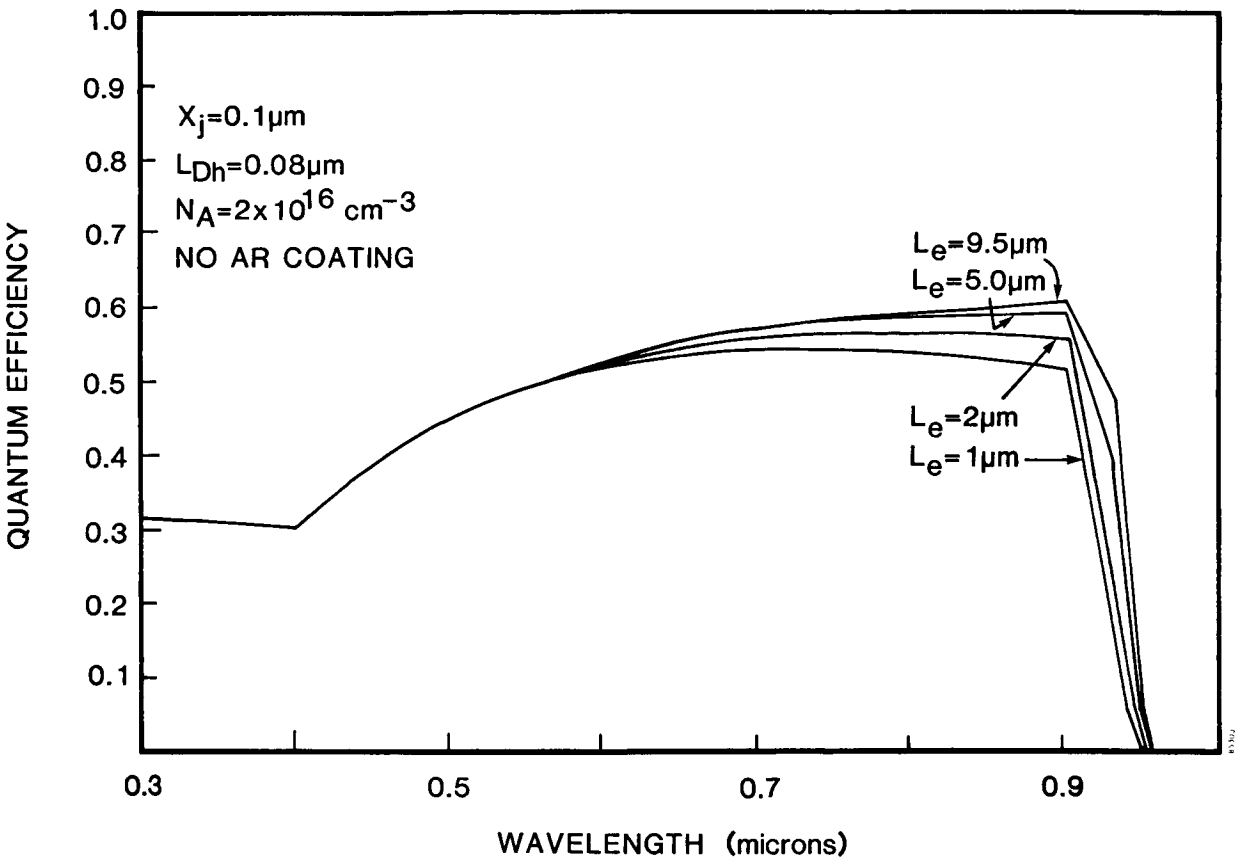

Figure 4. THEORETICAL EXTERNAL QUANTUM EFFICIENCY AS A FUNCTION OF WAVELENGTH AND BASE DIFFUSION LENGTHS.

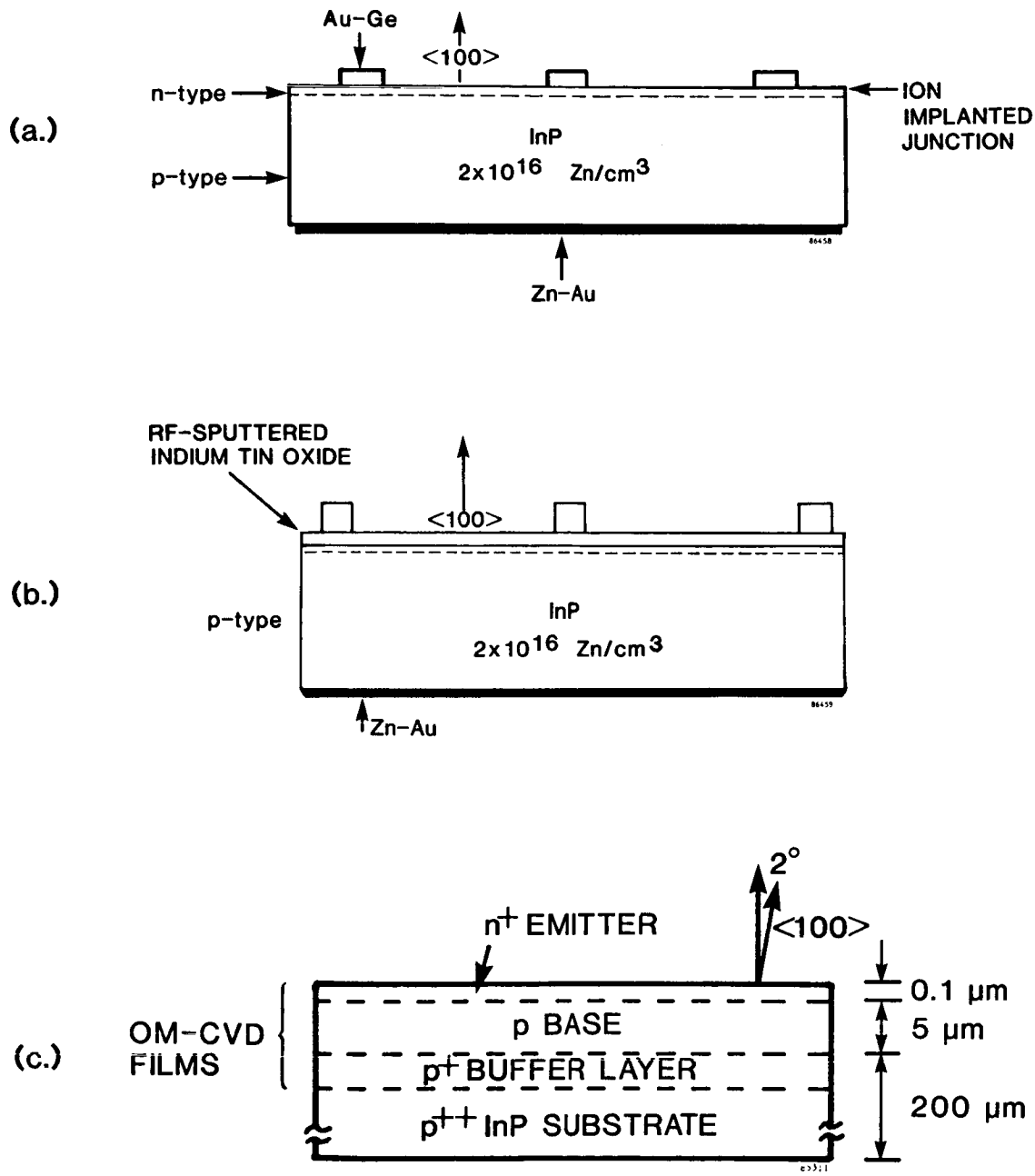

Figure 5. INDIUM PHOSPHIDE SOLAR CELL DESIGNS. (a) Ion-implanted cell, (b) Indium tin oxide coated cell, (c) Epitaxial cell.

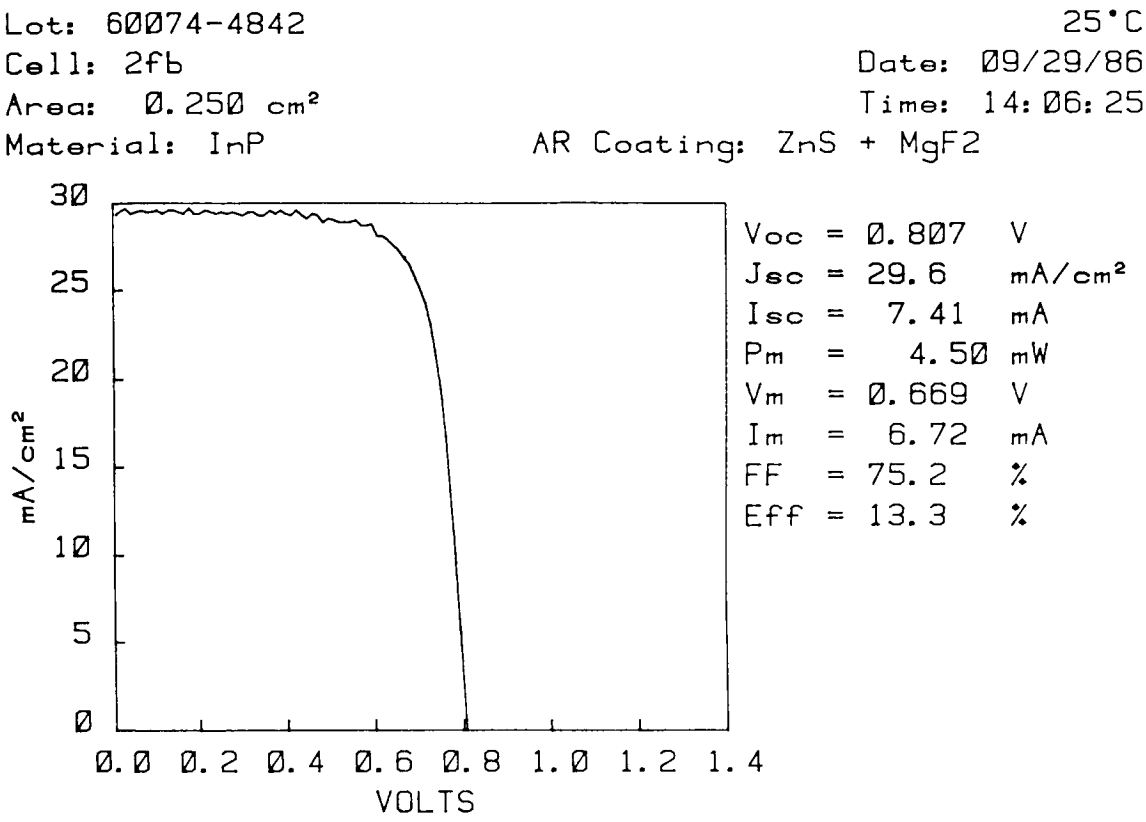

Figure 6. ILLUMINATED I-V CHARACTERISTIC FOR AN ION-IMPLANTED InP HOMOJUNCTION SOLAR CELL (AM0, 135 mW/cm^2)

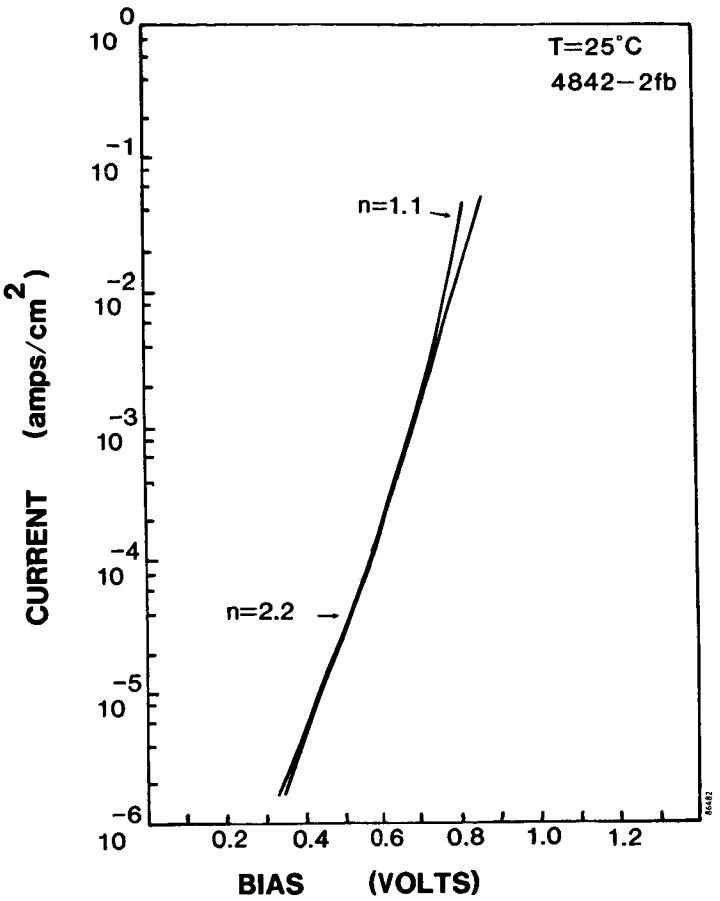

Figure 7. DARK LOG CURRENT VOLTAGE CHARACTERISTIC AND I_{sc} PLOT FOR DEVICE 4842-2fb

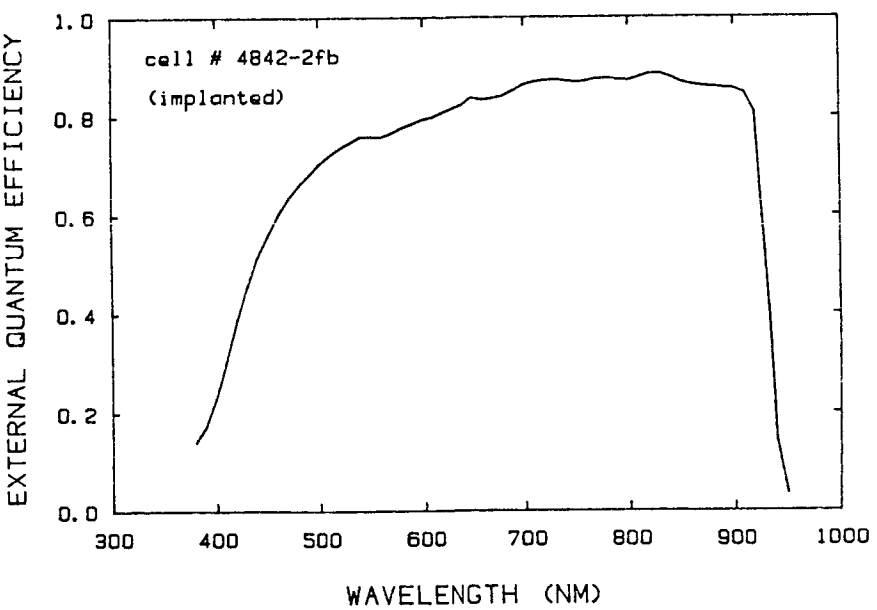

Figure 8. EXTERNAL QUANTUM EFFICIENCY OF DEVICE 4842-2fb